

Nanoscale

Accepted Manuscript



This is an *Accepted Manuscript*, which has been through the Royal Society of Chemistry peer review process and has been accepted for publication.

Accepted Manuscripts are published online shortly after acceptance, before technical editing, formatting and proof reading. Using this free service, authors can make their results available to the community, in citable form, before we publish the edited article. We will replace this *Accepted Manuscript* with the edited and formatted *Advance Article* as soon as it is available.

You can find more information about *Accepted Manuscripts* in the [Information for Authors](#).

Please note that technical editing may introduce minor changes to the text and/or graphics, which may alter content. The journal's standard [Terms & Conditions](#) and the [Ethical guidelines](#) still apply. In no event shall the Royal Society of Chemistry be held responsible for any errors or omissions in this *Accepted Manuscript* or any consequences arising from the use of any information it contains.

Cite this: DOI: 10.1039/c0xx00000x

www.rsc.org/xxxxxx

ARTICLE TYPE

Germanium-doped carbon dots as a new type of sensitive and selective fluorescent probe for visualizing the dynamic invasions of mercury (II) ions into cancer cells

Yun Huan Yuan,^a Rong Sheng Li,^b Qiang Wang,^b Zhu Lian Wu,^a Jian Wang,^b Hui Liu,^{*,b} and Cheng Zhi Huang^{*,a}

Received (in XXX, XXX) Xth XXXXXXXXX 20XX, Accepted Xth XXXXXXXXX 20XX

DOI: 10.1039/b000000x

Carbon dots doped with germanium (GeCDs) were firstly prepared by a new simple 15 min carbonation synthesis route, exhibiting excitation-independent photoluminescence (PL), which could avoid autofluorescence in bioimaging applications. The as-prepared GeCDs have low cell toxicity, good biocompatibility, high intracellular delivery efficiency, stability and could be applied for detection of mercury (II) ions with excellent selectivity in complicated medium. It is noted that the as-prepared GeCDs used as a new type of probe for visualization of dynamic invasions of mercury (II) ions into Hep-2 cells, displaying greatly different properties from most of previously reported CDs which are regularly responsive to irons. All the results denominate that the GeCDs can be employed for visualization and monitoring the significant physiological changes of living cells induced by Hg²⁺.

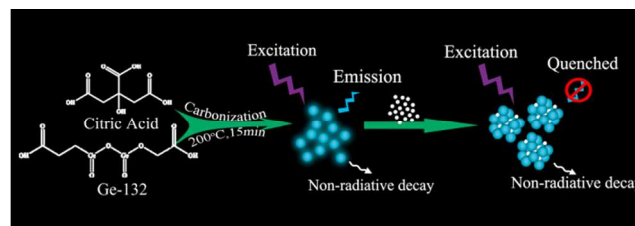
Introduction

Carbon dots (CDs), which generally refer to carbon nanomaterials less than 10 nm in size, have drawn increasing attention since the first discovery by Scrivens' group in 2004¹. CDs have gradually become a rising star in carbon-based luminescent nanomaterials owing to their interesting and unique features, such as easy preparation, high quantum yield, good photostability, excellent biocompatibility, and low toxicity, etc.^{2,3}. The potential of CDs in biomedical applications is enormous because they are generally nontoxic and originated from the common-employed and extensively existed carbon element^{4,5}. Therefore, CDs have been used for various purposes such as imaging, biosensing^{6,7}, biomedical research⁸, and new solar energy materials. For example, Ju *et al.* developed a simple indicator for detection of hydrogen peroxide in biological environments⁹, and Gao *et al.* demonstrated a new method of trace superoxide anion in live cells by using a carbon-dot-based ratiometric fluorescent probe¹⁰. It is still exciting for developing CDs with functional groups such as carboxyl, hydroxyl since they are not easy to be photobleached and have shown highly promising prospects in regard to nanosensors, bioimaging in live cells, tissues, and animals¹¹⁻¹³. These applications inspired us that developing new types of CDs could further improve the techniques such as biosensing and in vivo bioimaging.

Owing to the influence of electron, heteroatom doping into CDs has become a powerful approach to improve the photoluminescence properties of CDs, which obviously broadens their applications^{14,15}. For example, nitrogen-doped CDs showed not only high luminescence performance but also good biocompatibility¹⁶⁻¹⁸. Similarly, sulfur-doped CDs, silicon-doped CDs and boron-doped CDs displayed excellent

photoluminescence, low toxicity and excellent biocompatibility and have been used as fluorescent nanosensors or probes for imaging¹⁹⁻²¹. However, germanium, a member of group IV just like C and Si, which is more inclined to sp³-like bonding, is considered to influence the electronic and structural properties of carbon-based material in a different way compared with N or S doping²⁰, and thus we believe that germanium-doped carbon dots (GeCDs) deserves further investigations.

In this paper, we firstly report an easy bottom-up route (Scheme 1) to obtain the GeCDs by using citric acid and bis(2-carboxyethyl)germanium (IV) sesquioxide (Ge-132) as precursor. Compared to the previously reported route to prepare CDs, our present one only requires a simple carbonization procedure of 15 min, and the as-prepared GeCDs have low cell toxicity, good biocompatibility, high intracellular delivery efficiency, and stability. Furthermore, the as-prepared GeCDs are highly specific to Hg²⁺, which could be used for the detection of Hg²⁺ even if in extremely complicated medium, such as the honeysuckle dew samples. Particularly, the obtained GeCDs could be employed for



Scheme 1 Illustration of the formation process of GeCDs by carbonization and its further applications for Hg²⁺ detection.

imaging and monitoring the cellular activities of Hg^{2+} in Hep-2 cells. Hence, the GeCDs may have great potential as a high-performance platform for real-time tracking of Hg^{2+} in living cells.

5 Experimental

Apparatus

The fluorescence spectroscopy was recorded by an F-2500 fluorescence spectrophotometer (Hitachi, Tokyo, Japan) and the UV-vis absorption spectroscopy was obtained with a UV-3600 spectrophotometer (Hitachi, Tokyo, Japan). High-resolution TEM (HRTEM) images were performed with a high resolution transmission electron microscope (Tecnai G2 F20 S-TWIN, FEI Company, USA), which was operated at an accelerating voltage of 200 kV. Elemental and functional groups analysis was performed on a Thermo escalab 250Xi X-ray photoelectron spectrometer and a FTIR-8400S Fourier transform infrared spectrometer (Tyoto, Japan) respectively. Zeta potentials were obtained by dynamic laser light scattering (ZEN3600, Malvern). The Raman spectrum was obtained by LabRAM HR800 Laser confocal Raman spectrometer at ambient temperature (about 25 °C) on an Ag substrate. Absolute quantum yield was obtained by Absolute PL Quantum Yield Spectrometer C11347 (Hamamatsu, Japan). FL-TCSPC fluorescence spectrophotometer (Horiba Jobin Yvon Inc., France) was used to characterize the fluorescence life time. The thickness distribution of CDs was characterized by Multimode atomic force microscopy (AFM) measurements. X-ray diffraction (XRD) patterns were obtained using an Ultima IV instrument. Fluorescence imaging was operated on a DSU live-cell confocal microscope (Olympus, Japan) system with laser excitations of DAPI.

Synthesis of the photoluminescent carbon dots

The CDs were prepared by directly carbonizing CA and Ge-132. The specific procedure of CDs preparation, 0.2 g CA and 0.1 g Ge-132 were mixed fully and put into a 10 mL flask, and then the mixture was heated to 200 °C using a heating mantle. About 2 minutes later, this mixture was liquated. Subsequently, the liquid gradually turned into pale yellow liquated, and then yellow liquated in 15 min, indicating the formation of CDs. It is worth noting that there were water droplets and bubbles in the whole process. Next, pouring the 8 mL of 1.65 g/100 mL KOH solution into reactant for neutralizing the solution to pH 7.0, the aqueous solution of CDs was obtained. For XPS, prior to joining KOH solution, through a dialysis membrane (1000 MWCO), residual CA and Ge-132 will be removed.

45 Detection of Hg^{2+} ion

The detection of Hg^{2+} was performed at room temperature in Britton–Robinson buffer (BR buffer) (pH 7.0) solution. In a typical assay, 0.10 mL BR buffer (pH7.0) and 0.10 mL CDs were added into a 2.0 ml tube, followed by the addition of different concentrations of Hg^{2+} ion, and make them mixed fully, which was diluted to 1.00 mL with doubly distilled water and blended again. The photoluminescence (PL) emission spectra were recorded after reaction for 10 min at room temperature. The

selectivity for Hg^{2+} ion was confirmed by adding other metal ions solutions instead of Hg^{2+} ions in a similar way. The sensitivity and selectivity measurements were conducted in triplicate. The great sensitivity and selectivity of CDs to Hg^{2+} ions implying the feasibility of CDs for detecting Hg^{2+} in real samples. The honeysuckle dew obtained from Hubei Wushi Pharmaceutical. Before evaluating, the samples were filtered through a 0.22 μm membrane and then centrifuged at 12 000 rpm for 20 min. The honeysuckle dew samples were spiked with standard solutions at different concentrations of Hg^{2+} and then analyzed with the proposed method.

65 Cytotoxicity investigation

100 μL 1×10^5 cells per mL of Human epidermoid cancer cells (Hep-2) in Roswell Park Memorial Institute 1640 medium (RPMI 1640) supplemented with 2% fetal bovine serum were added to each well of a 96-well plate. The cells were cultured first for 24 h in an incubator (37 °C, 5% CO_2), and for another 24 h after the culture medium was replaced with 90 μL of RPMI 1640 containing 10 μL of the CDs at different doses (0, 0.2, 0.4, 0.6, 0.8, 1 mg mL^{-1}). For the cytotoxicity investigation of mercury (II) ions, the cells were incubated with same doses of CDs (1 mg mL^{-1}) for 24 h, then treated with different concentrations of mercury (II) ions (0, 2, 5, 10, 20 μM) for 30min. After removing the culture medium, the cells washed with PBS buffer twice, then 10 μL of Cell Counting Kit-8 (CCK-8) solution was added to every cell well, which were contained 90 μL RPMI 1640. The cells were further incubated for 1 h. The optical density (OD) of the mixture was measured at 450 nm with a Microplate Reader Model. The cell viability was estimated according to the following equation:

$$\text{Cell viability [\%]} = \frac{\text{OD treated}}{\text{OD control}} \times 100\%$$

Wherein OD control was obtained in the absence of CDs, and OD treated obtained in the presence of CDs.

Intracellular uptake experiment

The Hep-2 cells in RPMI 1640 supplemented with 10% fetal bovine serum were added to each well of a 24-well plate (300 μL per well). The cells were cultured first for 24 h in an incubator (37°C, 5% CO_2), and for another 12 h after the culture medium was replaced with 270 μL of RPMI 1640 containing 30 μL CDs (at the concentration of 1 mg mL^{-1}). Finally, followed removing the culture medium, each well was washed with PBS buffer for three times. For selective detection of mercury ions, the first group treated with PBS for 0, 10, 15, 20 and 30 min, the second group, the third group, fourth group and fifth group treated with PBS and 2, 5, 10, 20 μM mercury ions, respectively, for 0, 10, 15, 20 and 30 min, then mounted with glycerol on microscope slides for imaging.

100 Results and discussion

Characterizations of as-obtained CDs

Fig. 1a shows that the as-prepared GeCDs are mono-dispersed, and their average size is about 2.9 nm with a very narrow distribution between 2 and 4 nm. The high resolution TEM

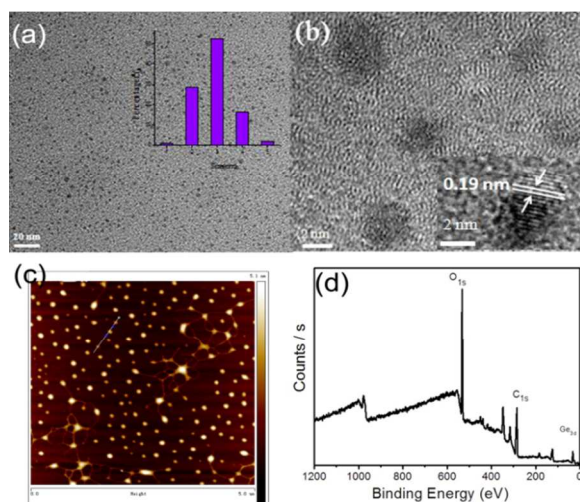


Fig.1 The morphology and the size distribution of the as-prepared GeCDs. (a) TEM image of CDs and (b) HRTEM images of the CDs. Inset: size distribution and HRTEM image of the CDs. The size distribution histogram was obtained by statistical analysis of more than 100 particles. (c) AFM image and height distribution of the CDs. (d) Full scan XPS spectrum of GeCDs.

(HRTEM) image (Inset of Fig. 1b) clearly shows the lattice spacing of 0.19 nm, which may be attributed to the (102) facet of graphitic carbon²². The XRD pattern of the CDs (Fig.S1, ESI†) displays a broad peak centered at 27°, similar to the graphite lattice spacing, which is attributed to highly disordered carbon atoms. The Raman spectrum of CDs illustrates two very prominent peaks at around 1356 cm⁻¹ and 1606 cm⁻¹. The former peak can be attributed to the disordered D-band due to sp³ carbons, while the latter peak can be attributed to the crystalline G-band due to sp² carbons (Fig. S4, ESI†). In conclusion, all the measurements of HRTEM, XRD and Raman are well consistent, indicating that the as-prepared CDs are composed of nanocrystalline cores of graphitic sp² carbon atoms and that there are sp³ carbons defects in the cores or on the surfaces. The AFM result shows that the height of the CDs varies from 2.5 nm to 3.1 nm (Fig. 1c), which approximates the average size of the CDs. The XPS measured to characterize the surface composition and elemental analysis showed that the full scan XPS spectrum (Fig. 1d) of the CDs displays the existence of carbon (C 1s, 285.78 eV), germanium (Ge 3d, 32.29 eV), and oxygen (O 1s, 532.01 eV), indicating that the Ge element (atomic percentage is 5.13) was doped into carbon dots successfully.

The absorption band at 3424 cm⁻¹ and 1393 cm⁻¹ in the FTIR spectrum of GeCDs indicates the existence of -OH, which can improve the hydrophilicity and stability of the GeCDs in the neutral and weak basic aqueous solution. The peaks at 2927 cm⁻¹ is attributed to C-H stretching vibrations, 1651 cm⁻¹ can be assigned to C=O stretching vibrations. The characteristic absorption band of C=C stretching at 1578 cm⁻¹ is also observed, and the absorption band at 1153 cm⁻¹ is assigned to C-O stretching vibrations (Fig. S3, ESI†). The zeta potential of the CDs in aqueous solution is -26.1 mV, indicating that the -COOH and -OH groups on the surface.

The aqueous dispersed GeCDs own unique optical properties.

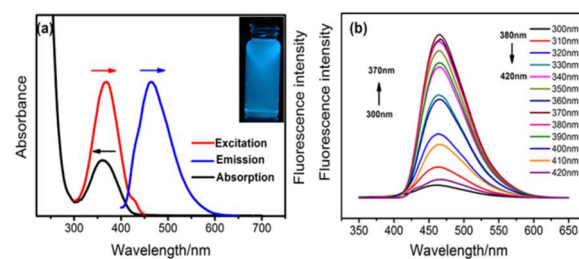


Fig. 2 UV-vis absorption and PL spectra of the GeCDs. (a) The emission spectrum (blue) was obtained under maximum excitation at 365 nm, and the excitation spectrum (red) was obtained at the maximum emission wavelength of 465 nm. The black curve shows the absorption spectrum of the as-prepared GeCDs. Inset: photograph taken under 365 nm UV light. (b) Emission spectra of CDs at different excitation wavelengths.

Owing to the $n \rightarrow \pi^*$ transition of C=O, the GeCDs displays a strong absorption band characterized at 361 nm (Fig. 2a), which is consistent with the maximum excitation wavelength at 365 nm. Therefore, the as-prepared GeCDs exhibit a bright blue-green color under the illumination of UV light (365 nm) (the inset photograph of Fig. 2a), and under the excitation of light with different wavelengths the emission of CDs is always kept at 465 nm (Fig. 2b). That is, the water-soluble GeCDs shows excitation-independent photoluminescent (PL) behaviour, which are greatly different from most previously reported CDs that are excitation-dependent photoluminescent^{11, 23}.

Here it should be noted that the excitation-independent emissions implies that both the size and the surface state of those CDs should be uniform, which can avoid autofluorescence during their applications²⁴. Meanwhile, the absolute quantum yield (QY) of the GeCDs approximately 8.9%, which is much higher than the 5.6% of those CDs prepared with only citric acid, indicating that the doping of germanium element can modify the emission ability of CDs. The possible reason might be attributed to influence of the doped germanium on the surface-trapped electrons and structural properties of the GeCDs. Furthermore, the as-prepared GeCDs only have one fluorescence lifetime of 1.54 ns (Fig. S5, ESI†), indicating that the excitation-independent photoluminescent could be ascribed to single transition mode²⁵. Since the lifetime is very short so that the fluorescence emissions might be attributed to radiative recombinations of the carbon particle surface-trapped electrons and holes²⁶, namely, the exciton emissions²⁷.

80 Stability of the as-prepared GQDs

We also designed a series of control experiments to examine the stability of the CDs. The fluorescence intensities are scarcely shows any change by varying the NaCl concentrations (up to 2 M), indicating the stability of the CDs even under comparatively high ionic-strength medium (Fig. S6, ESI†). Meantime, the CDs exhibit good photostability, PL intensity remains invariant under continuous UV light (365 nm) illumination for three hours (Fig. S7, ESI†). The PL intensity almost retains 82% of the initial fluorescence intensity after incubation with 100 mM H₂O₂ for 40 min (Fig. S8, ESI†). These points verify the CDs own very excellent stability, which laid a good foundation for future applications in bioimaging and detection.

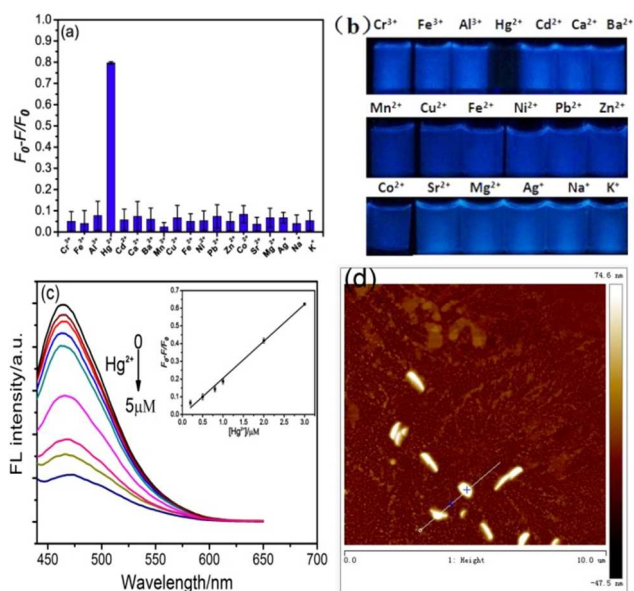


Fig. 3 The binding features of GeCDs with metal ions. (a) selective binding of GeCDs with mercury (II) ions, and no binding with other metals ions including iron ions; (b) photographs of the CDs containing various metal ions under UV light (excited at 365nm and the concentrations of Hg^{2+} and other metal ions were 5 μM). (c) Emission spectra of CDs in the presence of different concentrations of Hg^{2+} . Inset: the linear relationship between the PL intensity and Hg^{2+} concentration in the range of 0.2 μM and 3 μM , and there was a great linear calibration plot expressed as $(F_0 - F)/F_0 = 0.21c - 0.004$ with a correlation coefficient of 0.9968. (d) The AFM image of the as-prepared GeCDs with Hg^{2+} ions.

Detection the Hg^{2+} ion with excellent selectivity and sensitivity

It is very interesting that the GeCDs have specific binding ability with Hg^{2+} . As Fig 3a and 3b showed, there was significant PL quenching with the addition of Hg^{2+} into the CDs dispersion. In contrast, other metal ions including Cr^{3+} , Fe^{3+} , Al^{3+} , Cd^{2+} , Ca^{2+} , Ba^{2+} , Mn^{2+} , Cu^{2+} , Fe^{2+} , Ni^{2+} , Pb^{2+} , Zn^{2+} , Co^{2+} , Sr^{2+} , Mg^{2+} , Ag^+ , Na^+ and K^+ have no significant quenching effect. A significant observation is that the GeCDs have no any binding features with irons, greatly different from other CDs previously reported^{28, 29}.

The selective binding of GeCDs with Hg^{2+} deserves further discussion. Firstly, the PL intensity of the GeCDs at around 465 nm gets decreased with the increase of Hg^{2+} concentration (Fig. 3c) with a great linear plot in the range of 0.2 μM and 3 μM (Inset of Fig. 3c), and giving a limit of detection (LOD) about 0.075 μM with the three times the standard deviation rule ($\text{LOD} = 3\text{Sd}/s$), indicating that the GeCDs is very sensitive to Hg^{2+} . It should be noted that the obtained LOD the GeCDs sensor for Hg^{2+} detection is much lower than those previously reported, such as the QG compound and polymer sensor¹⁸. Then, the lifetime of the GeCDs gets changed with their binding with Hg^{2+} , which contains two lifetime components, 1.15 ns and 4.54 ns. The different values were might due to the aggregations of the CDs³⁰. In addition, we noticed that the height of the GeCDs get enlarged from 3 nm to 70 nm after the interaction between GeCD with Hg^{2+} (Fig. 3d), indicating that some aggregations have occurred. All these results illustrate that the fluorescence quenching might be induced by the special coordination interaction between Hg^{2+} ions and the hydroxyl or carboxyl groups on the surfaces of the GeCDs, leading to the aggregations

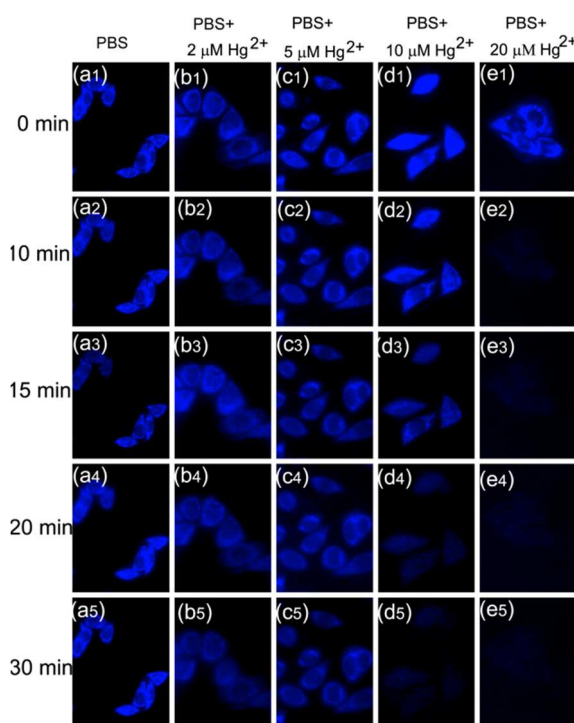


Fig.4 Laser confocal microscopic images of Hep-2 cells incubated with GeCDs for 12h. Then treated with PBS for 0, 10, 15, 20 and 30min, respectively (a₁, a₂, a₃, a₄ and a₅), PBS and 2 μM mercury ions for 0, 10, 15, 20 and 30min, respectively (b₁, b₂, b₃, b₄ and b₅), PBS with 5 μM mercury ions for 0, 10, 15, 20 and 30min, respectively (c₁, c₂, c₃, c₄ and c₅), respectively, PBS with 10 μM mercury ions for 0, 10, 15, 20 and 30min, respectively (d₁, d₂, d₃, d₄ and d₅), and PBS and 20 μM mercury ions for 0, 10, 15, 20 and 30min, respectively (e₁, e₂, e₃, e₄ and e₅).

of the CDs. That changes the electronic structure of GeCDs and exerts effects on the distribution of excitons, thus the non-radiative recombination of excitons through the charge transfer process could be facilitated and the fluorescence quenching of CDs could be occurred²⁴.

Considering that mercury (II) ion is one of the most toxic and widespread pollutants, which can cause a wide range of risks in human health and environmental conditions³¹, we made detections of Hg^{2+} in honeysuckle dew samples (Table.S1, ESI†) based on the photoluminescence of the GeCDs, showing that the selective detection of Hg^{2+} in real samples is reliable.

Cytotoxicity investigation

Due to their remarkable stability, the CDs are suitable for biological imaging. To demonstrate the possible cellular toxicity brought by doping Ge atoms, the MTT assay was carried out by Human epidermoid cancer cells. The CDs exhibit fairly low cytotoxicity even at high concentration (1 mg mL⁻¹) and after long incubation times (24 h), suggesting the doping of Ge atoms has little influence on cell toxicity of CDs (Fig. S9, ESI†). Therefore, the uptake of the CDs and bioimaging experiments were also made by confocal fluorescence microscope. Furthermore, a viability test was also carried out with the same concentrations bioimaging experiments of Hg^{2+} . It is seen that the cells viability decreased with increasing the concentrations of Hg^{2+} , especially when the concentration of mercury ions reached to 10 μM and 20 μM (Fig. S10, ESI†). This result is consistent

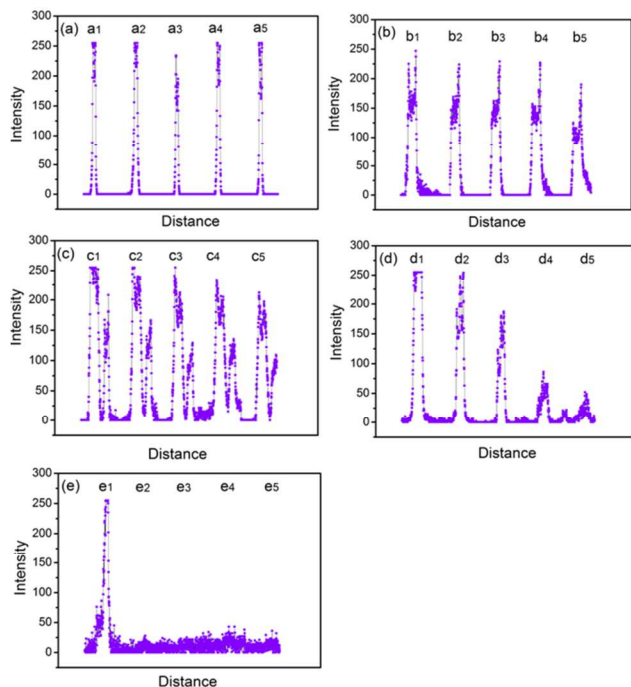


Fig.5 Quantitative analyzed of fluorescence intensity in each group of cell with result of the bioimaging.

Visualization of dynamic invasions of mercury (II) ions into Hep-2 cells

It has known that the excessive Hg^{2+} can easily enter bloodstreams and many tissues, such as liver, kidney, and brain, leading to kidney failure, gingivitis, and seriously damage to the central nervous system^{32, 33}, but not all concentrations of Hg^{2+} are significantly accelerated apoptosis of cells³⁴. Furthermore, real-time monitoring of physiological changes of cells caused by metal ions is such important for biological and biomedical research³⁵. In such case, Hep-2 cells were employed for investigating the cellular activities of Hg^{2+} .

Fig. 4a₁ shows that strong bright blue-green areas inside the Hep-2 cells are clearly observed after the cell incubated with GeCDs, suggesting that GeCDs successfully and efficiently got into cells via endocytosis³⁶. A further study at different time scales (0, 10, 15, 20 and 30 min) revealed that the fluorescence emissions scarcely changed with increasing time (Fig. 4a₁, a₂, a₃, a₄ and a₅), implying that the GeCDs are high resistant to photobleaching, and thus the GeCDs are an ideal candidate for real-time monitoring of the intracellular activities of mercury (II) ions with extended observation time.

Further experiments were performed by treating the cells with different concentrations of Hg^{2+} to examine their apoptosis in a short time. When incubated with 2.0 μM and 5.0 μM mercury (II) ions, respectively, the fluorescence emissions were not substantially quenched within 30 min (Fig. 4), indicating that a small amount of mercury (II) ions got into cells and apoptosis of the Hep-2 cells did not significantly occur (Fig. S11, ESI†). If treated with 10 μM mercury (II) ions, the photoluminescence signal gradually decayed with increasing time, which almost disappeared within 30 min (Fig. 4), implying the mercury (II) ions had got into the cells and apoptosis begun³⁷ (Fig. S11, ESI†).

Furthermore, the cells incubated with 20.0 μM mercury (II) ions, the fluorescence signal was rapidly quenched within 10 min (Fig. 4), demonstrating the apoptosis of the cells have been affected seriously (Fig. S11, ESI†). Certainly, cell viability assays with the same concentrations of Hg^{2+} and the quantitative analysis of the fluorescence intensity were also been carried out, which were consistent with the laser confocal microscopic images (Fig. S10, ESI† and Fig. 5). That is to say, the photoluminescence of CDs was rapidly and substantially quenched by 10.0 μM and 20.0 μM mercury (II) ions, providing clear evidence that mercury(II) ions has a significantly impact on the cell. In contrast, treatment of cells with Hg^{2+} less than 5.0 μM concentrations in a short time did not get significantly increase the proportion of apoptotic cells³⁴. Taken together, these findings revealed that the GeCDs can be employed for high selective visualization and monitoring the significant physiological changes of living cells induced by Hg^{2+} .

We also explored the location of nanoparticles in cells for further bioassays. Although there are many CDs distributed in lysosomes, the other organelles also have CDs (Fig. S12, ESI†), including golgi apparatus and endoplasmic reticulum. This is different from the QDs which mainly distributed in lysosomes³⁶, this might be attributed to the major component of CDs is the nontoxic element carbon and the CDs own good biocompatibility. The results demonstrated that the GeCDs have potential value for biological and biomedical research.

Conclusions

In summary, pyrolyzing citric acid and Ge-132 has been proven to be an effective strategy for fabricating fluorescent GeCDs for the first time. The as-prepared GeCDs are extremely stable and have low cytotoxicity, exhibiting great emission properties and excitation-independent PL emission behaviour, and thus successfully applied for the detection of Hg^{2+} in complicate sample such as in honeysuckle dew and the monitoring of the cellular activities of mercury (II) ions. It is believed that the new developed synthetic route for fabricating GeCDs could provide a new way for developing CDs with functional properties, and the excellent selectivity of the GeCDs for Hg^{2+} in complex samples has great potential for further understanding the cellular activities of heavy metal ions.

Acknowledgements

This work was financially supported by the National Natural Science Foundation of China (No. 21035005) and the Ministry of Science and Technology of the People's Republic of China (2011CB933600).

Notes and references

^a Education Ministry Key Laboratory on Luminescence and Real-Time Analysis, College of Chemistry and Chemical Engineering, Southwest University, Chongqing 400715, China. E-mail: chengzhi@swu.edu.cn, Tel: (+86) 23 68254659, Fax: (+86) 23 68367257.

^b College of Pharmaceutical Science, Southwest University, Chongqing 400716, China. E-mail: liuhui78@swu.edu.cn.

† Electronic Supplementary Information (ESI) available: Experimental section and additional figures (Fig.S1-S15). See DOI: 10.1039/b000000x/

1. X. Xu, R. Ray, Y. Gu, H. J. Ploehn, L. Gearheart, K. Raker and W. A. Scrivens, *J. Am. Chem. Soc.*, 2004, **126**, 12736-12737.
2. X. Li, S. Zhu, B. Xu, K. Ma, J. Zhang, B. Yang and W. Tian, *Nanoscale*, 2013, **5**, 7776-7779.
3. J. Zhou, Y. Yang and C.-y. Zhang, *Chem. Commun.*, 2013, **49**, 8605-8607.
4. S. K. Bhunia, A. Saha, A. R. Maity, S. C. Ray and N. R. Jana, *Sci. Rep.*, 2013, **3**, 1473.
5. W. Kong, J. Liu, R. Liu, H. Li, Y. Liu, H. Huang, K. Li, J. Liu, S.-T. Lee and Z. Kang, *Nanoscale*, 2014, **6**, 5116-5120.
6. W. Shi, X. Li and H. Ma, *Angew. Chem. Int. Ed.*, 2012, **51**, 6432-6435.
7. L. Shen, L. Zhang, M. Chen, X. Chen and J. Wang, *Carbon*, 2013, **55**, 343-349.
8. Y. Liu, Y. Xu, Y. Tian, C. Chen, C. Wang and X. Jiang, *Small*, 2014, **10**, 4505-4520.
9. J. Ju and W. Chen, *Anal. Chem.*, 2015, **87**, 1903-1910.
10. X. Gao, C. Ding, A. Zhu and Y. Tian, *Anal. Chem.*, 2014, **86**, 7071-7084.
11. K. Hola, Y. Zhang, Y. Wang, E. P. Giannelis, R. Zboril and A. L. Rogach, *Nano Today*, 2014, **9**, 590-603.
12. X. Gao, Y. Lu, R. Zhang, S. He, J. Ju, M. Liu, L. Li and W. Chen, *J. Mater. Chem. C*, 2015, **3**, 2302-2309.
13. S. Chen, J.-W. Liu, M.-L. Chen, X.-W. Chen and J.-H. Wang, *Chem. Commun.*, 2012, **48**, 7637-7639.
14. S. Qu, H. Chen, X. Zheng, J. Cao and X. Liu, *Nanoscale*, 2013, **5**, 5514-5518.
15. Y.-P. Sun, B. Zhou, Y. Lin, W. Wang, K. A. S. Fernando, P. Pathak, M. J. Meziani, B. A. Harruff, X. Wang, H. Wang, P. G. Luo, H. Yang, M. E. Kose, B. Chen, L. M. Veca and S.-Y. Xie, *J. Am. Chem. Soc.*, 2006, **128**, 7756-7757.
16. Z. L. Wu, P. Zhang, M. X. Gao, C. F. Liu, W. Wang, F. Leng and C. Z. Huang, *J. Mater. Chem.*, 2013, **1**, 2868-2873.
17. Z. L. Wu, M. X. Gao, T. T. Wang, X. Y. Wan, L. L. Zheng and C. Z. Huang, *Nanoscale*, 2014, **6**, 3868-3874.
18. R. Zhang and W. Chen, *Biosens. Bioelectron.*, 2014, **55**, 83-90.
19. S. Chandra, P. Patra, S. H. Pathan, S. Roy, S. Mitra, A. Layek, R. Bhar, P. Pramanik and A. Goswami, *J. Mater. Chem.*, 2013, **1**, 2375-2382.
20. Z. Qian, X. Shan, L. Chai, J. Ma, J. Chen and H. Feng, *ACS Appl. Mater. Interfaces*, 2014, **6**, 6797-6805.
21. P. Shen and Y. Xia, *Anal. Chem.*, 2014, **47**, 5323-5329.
22. S. Sahu, B. Behera, T. K. Maiti and S. Mohapatra, *Chem. Commun.*, 2012, **48**, 8835-8837.
23. H. X. Zhao, L. Q. Liu, Z. D. Liu, Y. Wang, X. J. Zhao and C. Z. Huang, *Chem. Commun.*, 2011, **47**, 2604-2606.
24. Y. Guo, Z. Wang, H. Shao and X. Jiang, *Carbon*, 2013, **52**, 583-589.
25. S. Y. Lim, W. Shen and Z. Gao, *Chem. Soc. Rev.*, 2015, **44**, 362-381.
26. P. Anilkumar, X. Wang, L. Cao, S. Sahu, J.-H. Liu, P. Wang, K. Korch, K. N. Tackett II, A. Parenzan and Y.-P. Sun, *Nanoscale*, 2011, **3**, 2023-2027.
27. J. Yao, M. Yang and Y. Duan, *Chem. Rev.*, 2014, **114**, 6130-6178.
28. Y. Zhai, Z. Zhu, C. Zhu, J. Ren, E. Wang and S. Dong, *J. Mater. Chem. B*, 2014, **2**, 6995-6999.
29. X. Yang, Y. Zhuo, S. Zhu, Y. Luo, Y. Feng and Y. Dou, *Biosens. Bioelectron.*, 2014, **60**, 292-298.
30. X. Qiu, S. Han, Y. Hu and B. Sun, *Chem-Eur. J.*, 2015, **21**, 4126-4132.
31. A. Renzoni, F. Zino and E. Franchi, *Environ. Res.*, 1998, **77**, 68-72.
32. L. Deng, X. Ouyang, J. Jin, C. Ma, Y. Jiang, J. Zheng, J. Li, Y. Li, W. Tan and R. Yang, *Anal. Chem.*, 2013, **85**, 8594-8600.
33. G. Zhu, Y. Li and C.-y. Zhang, *Chem. Commun.*, 2014, **50**, 572-574.
34. F. J. Dieguez-Acuña, W. W. Polk, M. E. Ellis, P. L. Simmonds, J. V. Kushleika and J. S. Woods, *Toxicol. Sci.*, 2004, **82**, 114-123.
35. L. Qiu, T. Zhang, J. Jiang, C. Wu, G. Zhu, M. You, X. Chen, L. Zhang, C. Cui, R. Yu and W. Tan, *J. Am. Chem. Soc.*, 2014, **136**, 13090-13093.
36. K. Kantner, S. Ashraf, S. Carregal-Romero, C. Carrillo-Carrion, M. Collot, P. del Pino, W. Heimbrodt, D. J. De Aberasturi, U. Kaiser, L. I. Kazakova, M. Lelle, N. M. de Baroja, J. M. Montenegro, M. Nazareno, B. Pelaz, K. Peneva, P. R. Gil, N. Sabir, L. M. Schneider, L. I. Shabarchina, G. B. Sukhorukov, M. Vazquez, F. Yang and W. J. Parak, *Small*, 2015, **11**, 896-904.
37. J. Tian, L. Ding, H. Ju, Y. Yang, X. Li, Z. Shen, Z. Zhu, J.-S. Yu and C. J. Yang, *Angew. Chem. Int. Ed.*, 2014, **53**, 9544-9549.